NEW IMPACT CRATERS ON MARS SINCE THE LANDING OF THE INSIGHT MISSION.

K. Miljković[1], I. J. Daubar[2], A. Rajsic[1], T. Neidhart[1], E. K. Sansom[1], G. S. Collins[3], N. Wojcicka[3], N. A. Teanby[4], M. E. Banks[5], L. Posiolova[6], M. Malin[6], [1]Curtin University, School of Earth and Planetary Science, Perth, Australia (katarina.miljkovic@curtin.edu.au), [2]Brown University, Providence, RI, USA, [3]Imperial College London, UK, [4]Bristol University, UK, [5]NASA Goddard Space Flight Center, USA, [6]MSSS, San Diego, CA, USA.

Introduction: NASA's InSight mission has been operating on Mars for over 2 years [1]. In the first year of operations, the seismometer SEIS (Seismic Experiment for Interior Structure) recorded hundreds of quakes [2]. The number of recorded quakes is increasing on a daily basis. However, none of the seismic events has been confidently identified to have originated from an impact event to date. One impact event created a 1.5 m diameter crater about 37 km from the InSight lander (light blue marker in Figure 1, HiRISE image ESP_060062_1840). It was close to the detectability limit but could not definitively be linked to any of the three isolated seismic signatures that occurred in the possible time period of the impact [3].

Explanations as to why there have not yet been any impacts confidently identified by SEIS could be: a) unfavorable impact bombardment statistics in terms of their size and distance from InSight, b) the uppermost crust on Mars could be more dissipative towards seismic waves than previously thought [3], and/or c) the coupling between the impact energy and seismic generation is different on Mars than observed on the Moon [4-5, also see 6-7 at this conference]. Point (c) includes issues associated with impactor drag, ablation and fragmentation in the atmosphere that create different impact mechanics on Mars compared to the Moon. Points (b) and (c) could have caused lower seismic efficiencies than originally estimated [8-10], which lowers the detectability and reduces the surface area surrounding InSight over which impacts can be detected.

In this work, we discuss impact events that the Mars Reconnaissance Orbiter's HiRISE and CTX imaging teams have identified to have occurred on Mars since InSight's landing and why those were not detected by the seismometer on InSight.

Methods: All new impacts discussed here are available in the public HiRISE catalogue (https://www.uahirise.org/). The images were investigated in the HiView software package. Each crater was classified as a single or cluster of craters. The largest crater diameter was measured and, in the case of clusters, the approximate number of individual craters per cluster. The reason to measure the largest crater in a cluster is because the seismic signature of crater clusters is dominated by the largest crater in the cluster at large epicentral distances [11].

Analysis of the impact craters is shown in Figure 1 and Table 1. About 50% of the observed craters were likely single impacts (blue circles, Figure 1) and the other 50% were evidently cluster craters (grey squares) with less than 40 individual craters in the largest cluster. The largest single crater was ~14 m in diameter, and the largest crater in a cluster was ~13 m. The smallest resolvable crater was 1 m (pixel scale of the HiRISE data is about 20-30 cm/px). Except for the only impact that had a possibility of being detected by SEIS (1.5 m at 37 km distance, marked by light blue circle in Figure 1 and analysed by [3]), all other impacts occurred at 3000 to 8400 km distance from the InSight lander. The time window between the CTX images before and after the impacts was as little as 1-2 months, up to as long as 17 months. The longer the time window, the harder it is to interrogate the seismic data for an impact event.

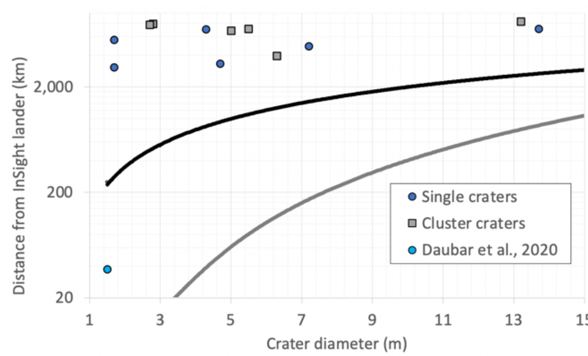

Figure 1: New impact craters as detected by the CTX and HiRISE to have occurred since the InSight landing, showing their crater diameter (x axis) and distance (y axis) from InSight. The black [9-10] and grey lines [4] show the estimated detection thresholds, for the low-noise (night time [12]) observations on Mars.

Figure 1 shows the crater diameter (or the largest crater in the case of a cluster of craters) on the x axis and the location of new craters expressed as distance from the InSight lander on the y axis. Figure 1 summarizes the impact detection threshold on Mars (here showing the case for the low ambient noise (at night time) on Mars [12]). Impacts could be identified in the seismic data if the impact crater size and distance from InSight falls below the black or grey lines. The black line is the scaling calculated before InSight landing [9-10] and the grey line is the recently updated detectability from numerical impact modelling [4]. The light blue marker is the impact crater that occurred close to the InSight lander (within ~37 km) and was borderline detectable [3-4]. All other impact events that have occurred on Mars post landing of InSight have so far been much further away from SEIS; They are one to two orders of magnitude too distant to be detectable.

Conclusions: None of the dozen known new impacts were detected by InSight because they occurred much too far away, consistent with detectability threshold estimates. Only one small crater as reported in [3] could have been recorded since the InSight landing.

Because orbital imaging is limited in space and time, these known new impacts represent only a fraction of the total number of impacts that have occurred on Mars in the last ~2 years. Based on previously observed bombardment rates [13], more than two hundred impacts >4 m in diameter occur on Mars each year. Extending that down to the smallest possibly detectable craters, [9] predicts ~3000 new craters >1 m in diameter have formed on Mars since InSight landed. If any of these unobserved impacts have been large enough and close enough to InSight to detect seismically, we have not yet discerned them in the seismic data.

Acknowledgments: KM, AR, and TN are supported by the Australian Research Council (DP180100661, DE180100584).

References: [1] Banerdt, W.B. et al. (2020) *Nature Geosci.* 13, 183-189. [2] Giardini, D. et al. (2020) *Nature Geosci.* 13, 205-212. [3] Daubar, I.J. et al. (2020) *J. Geophys. Res. Planets*, 125: e2020JE006382. [4] Wójcicka, N. et al. (2020) *J. Geophys. Res. Planets*, 125, e2020JE006540. [5] Rajšić et al. (2021) *J. Geophys. Res. Planets*, in review [6] Wójcicka, N. et al. (2021) *LPSC*, this issue. [7] Rajšić et al. (2021) *LPSC*, this issue. [8] Daubar, I.J. et al. (2018) *Space Sci. Rev.* 214, 132, 68 pp. [9] Teanby, N.A. & Wookey, J. (2011) *PEPI* 186, 70-80. [10] Teanby, N.A. et al. (2015) *Icarus* 256, 46-62. [11] Schmerr N.C. et al. (2019) *J. Geophys. Res: Planets*, 124, 3063-3081. [12] Lognonné, P. et al. (2020) *Nature Geosci*. 13, 213-220. [13] Daubar et al. (2013) *Icarus* 225, 506-516.

Table 1. Impact craters observed by Mars Reconnaissance orbiter, CTX and HiRISE, including our analysis of the impact type; the crater diameter, or the largest crater diameter in case of a cluster of craters; the time window in which the impact occurred according to CTX before and after images, and the distance from the InSight lander.

HiRISE observation ID	Lat	Lon (E)	Before image ID (CTX)	After image ID (CTX)	Time window (months)	Distance from InSight (km)	Largest crater diameter (m)	Impact type
ESP_059453_1335	-46.2097	208.6446	K12_058174_1341_XI_45S151W_181224	K15_059242_1334_XN_46S151W_190317	3.0	4,832	7.2	single
ESP_059728_1740	-5.8284	254.8211	K12_058238_1746_XI_05S105W_181229	K14_059016_1745_XN_05S105W_190228	2.1	7,066	5.5	cluster
ESP_060304_2135	33.3656	4.7771	K13_058392_2112_XN_31N354W_190110	K16_059737_2159_XI_35N355W_190425	3.0	7,104	13.7	single
ESP_061859_1785	-1.4930	41.1851	K15_059182_1792_XI_00S318W_190312	K17_060171_1792_XI_00S318W_190529	2.0	5,593	1.7	single
ESP_063433_2075	27.4086	261.1571	K20_061165_2077_XI_27N098W_190814	K22_061864_2077_XI_27N098W_191007	2.0	7,014	4.3	single
ESP_063930_2125	32.193	11.766	K21_061583_2122_XN_32N348W_190916	N01_062862_2121_XN_32N348W_191224	3.0	6,824	5	cluster
ESP_063953_2275	47.392	101.868	K19_060696_2263_XI_46N257W_190708	N04_063742_2260_XN_46N257W_200302	8.1	3,062	1.4	single
ESP_064880_1920	12.0638	359.1007	K13_058366_1892_XI_09N000W_190108	K18_060212_1941_XN_14N001W_190601	5.0	7,910	2.8	cluster
ESP_065387_1805	0.52	202.27	K19_060653_1834_XN_03N158W_190705	N03_063554_1791_XI_00S157W_200216	7.2	3,945	6.3	cluster
ESP_065843_1775	-2.72	354.86	K19_060898_1775_XN_02S005W_190724	N02_063021_1778_XN_02S005W_200106	6.1	8,330	13.2	cluster
ESP_066176_1790	-1.08	267.03	N06_064712_1801_XN_00N093W_200516	N08_065345_1801_XN_00N093W_200705	2.0	7,771	2.7	cluster
ESP_066551_1300	-49.75	119.7	K16_059720_1299_XN_50S240W_190423	N10_066208_1305_XI_49S240W_200910	17.3	3,312	4.7	single
ESP_060062_1840	3.866	135.613	K14_068929_1845_XN_04N224W_190221	K16_059495_1829_XN_02N224W_190406	1.5	37	1.5	single